Journal of Cerebral Blood Flow & Metabolism (2010) 30, 1200–1213

www.jcbfm.com

Evaluation of cerebral acetate transport and metabolic rates in the rat brain *in vivo* using ^{1}H-[^{13}C]-NMR

Anant B Patel[1,2], Robin A de Graaf[1], Douglas L Rothman[1], Kevin L Behar[3] and Graeme F Mason[1,3]

[1]*Department of Diagnostic Radiology, Magnetic Resonance Research Center, Yale University School of Medicine, New Haven, Connecticut, USA;* [2]*NMR Microimaging and Spectroscopy, Centre for Cellular and Molecular Biology, Hyderabad, India;* [3]*Department of Psychiatry, Magnetic Resonance Research Center, Yale University School of Medicine, New Haven, Connecticut, USA*

Acetate is a well-known astrocyte-specific substrate that has been used extensively to probe astrocytic function *in vitro* and *in vivo*. Analysis of amino acid turnover curves from ^{13}C-acetate has been limited mainly for estimation of first-order rate constants from exponential fitting or calculation of relative rates from steady-state ^{13}C enrichments. In this study, we used ^{1}H-[^{13}C]-Nuclear Magnetic Resonance spectroscopy with intravenous infusion of [2-^{13}C]acetate-Na^{+} *in vivo* to measure the cerebral kinetics of acetate transport and utilization in anesthetized rats. Kinetics were assessed using a two-compartment (neuron/astrocyte) analysis of the ^{13}C turnover curves of glutamate-C4 and glutamine-C4 from [2-^{13}C]acetate-Na^{+}, brain acetate levels, and the dependence of steady-state glutamine-C4 enrichment on blood acetate levels. The steady-state enrichment of glutamine-C4 increased with blood acetate concentration until 90% of plateau for plasma acetate of 4 to 5 mmol/L. Analysis assuming reversible, symmetric Michaelis–Menten kinetics for transport yielded 27 ± 2 mmol/L and 1.3 ± 0.3 μmol/g/min for K_t and T_{max}, respectively, and for utilization, 0.17 ± 0.24 mmol/L and 0.14 ± 0.02 μmol/g/min for K_{M_util} and V_{max_util}, respectively. The distribution space for acetate was only 0.32 ± 0.12 mL/g, indicative of a large excluded volume. The astrocytic and neuronal tricarboxylic acid cycle fluxes were 0.37 ± 0.03 μmol/g/min and 1.41 ± 0.11 μmol/g/min, respectively; astrocytes thus comprised $\sim$21% $\pm$ 3% of total oxidative metabolism.
Journal of Cerebral Blood Flow & Metabolism (2010) **30,** 1200–1213; doi:10.1038/jcbfm.2010.2; published online 3 February 2010

Keywords: brain acetate transport and utilization; fatty acids; glutamate; glutamine; nuclear magnetic resonance spectroscopy; neuron-glia trafficking

Introduction

Although glucose is the major energy substrate in the matured brain, substantial use of alternate fuels (e.g., ketone bodies, short- and medium-chain free fatty acids) may occur under certain conditions, such as fasting or starvation. Acetate, the smallest member of this group, has long been known to be oxidized by brain cells *in vivo* and *in vitro* (van den Berg and Garfinkel, 1971) and preferentially by astrocytes (Minchin and Beart, 1975). Studies of cultured cells have shown that acetate is preferentially transported and metabolized by astrocytes, whereas transport (and thus metabolism) in neurons is minimal (Waniewski and Martin, 1998). Acetate metabolism by astrocytes is strongly supported by ^{13}C isotopic labeling kinetics and ^{13}C isotopomer patterns of cerebral amino acids labeled from ^{13}C-acetate (Cerdán *et al*, 1990; Sonnewald *et al*, 1993). ^{13}C-Nuclear Magnetic Resonance (NMR) spectra obtained *in vivo* from rat and human brain during intravenous infusions of [2-^{13}C]acetate show substantial incorporation of ^{13}C in cerebral amino acids with higher enrichment in glutamine than glutamate (Cerdán *et al*, 1990; Lebon *et al*, 2002; Patel *et al*, 2005). These findings are consistent with acetate metabolism linked to a small and rapidly turning over cellular pool of glutamate, the latter serving as precursor to glutamine, supporting results of early studies using

Correspondence: Dr AB Patel, NMR Microimaging and Spectroscopy, Centre for Cellular and Molecular Biology, Uppal Road, Hyderabad, India.
E-mail: abpatel@ccmb.res.in
Received 9 September 2009; revised 16 December 2009; accepted 18 December 2009; published online 3 February 2010

^{14}C isotopes (van den Berg and Garfinkel, 1971). In a recent autoradiography study in nonstimulated awake rats, cerebral acetate utilization was estimated to be ~15% to 25% of total glucose consumption (Cruz *et al*, 2005).

As a specific probe of astrocytic metabolism, ^{13}C-NMR studies using singly or doubly ^{13}C-labeled acetate ([2-^{13}C], [1-^{13}C], [1,2-$^{13}C_2$]) in cultured astrocytes (Hassel *et al*, 1994), astrocytes/neuron cocultures (Brand *et al*, 1997), brain tissue slices (Badar-Goffer *et al*, 1990), and *in vivo* (Deelchand *et al*, 2009*b*; Lebon *et al*, 2002; Patel *et al*, 2005) have provided unique insights into astrocyte compartmentation and astrocyte/neuron trafficking of neurotransmitter precursors. A particularly valuable application of [2-^{13}C]acetate *in vivo* is the quantitative assessment of astrocytic tricarboxylic acid (TCA) cycle (V_{tcaA}) and glutamate/glutamine neurotransmitter cycle rates based on the analysis of steady-state ^{13}C enrichments of glutamine-C4 and glutamate-C4 (Lebon *et al*, 2002). The steady-state experiment allows acetate transport to be ignored, simplifying the analysis, but limiting information content to the ratio of two rates, $V_{cycle\_GluGln}/V_{tcaN}$. Additional information, e.g., time courses from [1-^{13}C]glucose, is required to calculate the absolute rates. A wealth of rate information resides within the ^{13}C dynamic time courses of the brain amino acid pools, which is accessible, in principal, with metabolic modeling in the manner used for ^{13}C-labeled glucose.

The major entry point for [2-^{13}C]acetate into cerebral metabolism is its conversion to acetyl-CoA-C2 by acetyl-CoA synthetase. The condensation of acetyl-CoA with oxaloacetate leads to formation of citrate and hence entry into the TCA cycle and labeling of α-ketoglutarate-C4. The ^{13}C label from α-ketoglutarate-C4 exchanges into glutamate-C4 by transamination through aspartate aminotransferase or reductive amination by glutamate dehydrogenase, followed by conversion to glutamine-C4 by the astrocytes-specific glutamine synthetase. Further metabolism of α-ketoglutarate-C4 in the second and subsequent turns of the astrocytic TCA cycle labels C2 and C3, which results in labeling of glutamate (and glutamine) -C2 and -C3 with eventual loss of label as CO_2. Mathematical analysis of the dynamic ^{13}C turnover curves of cerebral amino acids from plasma ^{13}C-acetate requires knowledge of the kinetics of acetate transport in brain *in vivo,* for which little information is currently available. Recently [2-^{13}C]acetate-Na^+ was infused to measure kinetics of acetate transport and consumption (Deelchand *et al*, 2009*b*), although further metabolism of the ^{13}C through the observed labeling of glutamate and glutamine was not evaluated. In another study [1,6-^{13}C]glucose and [1,2-$^{13}C_2$]acetate-Na^+ were used, but cerebral metabolic rates were also not evaluated (Deelchand *et al*, 2009*a*). The objective of this study is to investigate the kinetics of acetate transport and metabolism *in vivo*, simultaneously with evaluation of oxidative metabolism and glutamate–glutamine cycling. The analysis of data obtained using steady-state and transient ^1H-[^{13}C]-NMR measurements shows that acetate utilization in halothane anesthetized rat brain is capped primarily by metabolism and not by transport, but that transport significantly slows this process at physiologic concentrations of blood acetate.

Materials and methods

Animal Preparation

All animal experiments were performed in accordance with protocols approved by the Yale Animal Care and Use Committee. Overnight fasted Sprague Dawley rats (160 to 180 g) were anesthetized with halothane, tracheotomized, and artificially ventilated (30%O_2/68.5%N_2O, 1.5% halothane). Femoral arterial and venous catheters were placed for measurement of blood gases, blood pressure, and the infusion of [2-^{13}C]acetate-Na^+ and unlabeled glucose. Animals were placed in a small plastic cradle and a surface transceiver coil positioned on the scalp insulated by a layer of Saran Wrap. The animal and probe assembly were placed in the magnet bore with coil center placed at the isocenter of the magnet.

Experimental Study Groups

Group 1: Time courses of ^{13}C labeling of cortical metabolites were measured *in vivo* at 7.05 T during coinfusion of [2-^{13}C]acetate-Na^+ and unlabeled glucose ($n=6$). Details of infusion schedule are given in the infusion of substrates. The final rate of the acetate-Na^+ infusion was 0.25 mmol/kg/min. Arterial blood was sampled periodically for analysis of plasma acetate concentration and ^{13}C enrichment.

Group 2: Steady-state glutamine-C4 enrichments were determined *ex vivo* in bench experiments in rats infused with [2-^{13}C]acetate-Na^+ and unlabeled glucose for 40 min ($n=15$). For these measurements 40 min time was chosen based on *in vivo* experiments conducted in Group 1, which indicated that Gln-C4 labeling has been reached to steady state by this time (Figure 3E). Five different plasma acetate concentrations were produced (three rats studied per level) by adjusting the infusion rate. The final rates of acetate-Na^+ infusion used in these studies were 0.05, 0.10, 0.15, 0.25, and 0.50 mmol/kg/min. The glucose infusion protocol was the same in all experiments. At the conclusion of the infusion, the brain was frozen *in situ* using liquid N_2. Aqueous extracts of the cortex were subsequently prepared for analysis of ^{13}C-labeled metabolites.

Group 3: Time courses of the concentrations and C4 and C3 enrichments of glutamate and glutamine were determined *ex vivo* in bench experiments with infusion of [2-^{13}C]acetate-Na^+ and unlabeled glucose for 7 min ($n=4$) and 20 min ($n=4$). The final rate of acetate-Na^+ infusion was 0.25 mmol/kg/min. The brain was frozen *in situ* with liquid N_2 at the conclusion of the infusion. ^{13}C labeling of cerebral metabolites was measured in aqueous extracts of the cortex.

Infusion of Substrates

After the acquisition of baseline spectra, an intravenous infusion of [2-^{13}C]acetate-Na^+ (99 atom%, Cambridge Isotopes, Andover, MA, USA) and unlabeled glucose as described earlier (Fitzpatrick *et al*, 1992) was begun. [2-^{13}C]acetate-Na^+ was infused using a bolus-variable rate infusion (3 mol/L dissolved in water, pH adjusted to 7.0) at 1.25 mmol/min/kg (0 to 5 min), 0.625 mmol/min/kg (5 to 10 min), and 0.25 mmol/min/kg (final) thereafter until the end of the experiment. In Group 2 studies in which final infusion rates were changed, the rates of acetate-Na^+ used in the bolus (0 to 5 min) and middle steps (5 to 10 min) were also adjusted in same proportion. To maintain comparability with previous [1-^{13}C]glucose studies, unlabeled glucose was infused through a catheter in the opposite femoral vein according to a protocol described earlier (Patel *et al*, 2005) for all levels of acetate.

NMR Spectroscopy *In Vivo*

NMR experiments conducted *in vivo* were performed on a 7.05 T Bruker magnet interfaced with Avance spectrometer console (Bruker Instruments, Billerica, MA, USA) equipped with a 12-cm diameter actively shielded gradient coil insert (190 mT/m in 200 μsecs). ^{1}H NMR data were acquired with a 13-mm diameter surface coil transceiver operating at the resonance frequency (300.3 MHz). Two orthogonal 21-mm diameter coils tuned to the ^{13}C resonance frequency (75.5 MHz) and driven in quadrature served for transmission of inversion and decoupling pulses at the ^{13}C frequency.

Spatially localized ^{1}H and ^{1}H-[^{13}C]-NMR spectra were acquired serially (45 s per spectrum) to generate time courses of total metabolite levels and ^{13}C labeling as described earlier (de Graaf *et al*, 2003). Briefly, the position of the spectroscopic volume-of-interest was determined by acquiring three orthogonal fast gradient-echo images of the brain. Automated adjustments of first and second-order shims within a volume of $7 \times 7 \times 7\,mm^3$ using FASTMAP (Gruetter, 1993) resulted in water ^{1}H line widths 11 to 13 Hz. Three-dimensional localization ($7 \times 4 \times 7\,mm^3$) was achieved with a combination of outer-volume suppression, image selective *in vivo* spectroscopy, and slice-selective signal excitation techniques for the excitation and refocusing pulses. On alternate scans, radiofrequency was applied at the ^{13}C frequency with an echo delay that achieves selective inversion of resonances of protons coupled to ^{13}C; on subtraction of alternate scans, only resonances of ^{13}C-coupled protons such as glutamate remain. Water was suppressed using Selective Water Suppression with Adiabatic Modulated Pulse.

Processing of NMR Data Acquired *In Vivo*

Free induction decays were zero filled to 8192 data points, apodized (2.0 Hz Gaussian line broadening), Fourier transformed, and phase corrected. The ^{1}H-[^{13}C]-NMR difference spectrum was obtained by subtracting the ^{13}C-inverted spectrum (^{12}C−^{13}C) from the noninverted (^{12}C + ^{13}C) spectrum leaving only the ^{13}C-coupled ^{1}H resonances at twice their true intensity. Spectra were summed over 3 min intervals to increase the signal-to-noise ratio. Resonance intensities were measured using a linear combination algorithm adapted for independent labeling of carbon positions (de Graaf *et al*, 2003), which were then used to calculate the ^{13}C enrichment and concentration of metabolites.

Analysis of Plasma Acetate Concentration and Enrichment

Acetate concentration and isotopic ^{13}C enrichment were measured in the plasma isolated from arterial blood samples using ^{1}H NMR spectroscopy at 500 MHz (Bruker AVANCE, Bruker Instruments). The plasma samples were mixed with D_2O containing sodium formate and passed through a centrifugal filter (10 kDa cut off, Nanosep, Gelman Laboratory, MN, USA) to remove macromolecules. The percentage ^{13}C enrichment of [2-^{13}C]acetate in plasma (1.93 p.p.m.) was determined from the fully relaxed ^{1}H NMR spectrum (1.93 p.p.m.) and calculated by dividing the intensities of the two ^{13}C satellites by the total (^{12}C + ^{13}C) intensity. The concentration of acetate was determined relative to formate.

Preparation of Cortical Extracts

Metabolites were extracted from frozen fronto-parietal cortical tissue (150 to 200 mg) as described earlier (Patel *et al*, 2005). Frozen tissue was pulverized with ice-cold 0.1 mol/L HCl in methanol (1:2 wt/vol) in a dry-ice/ethanol bath and transferred to a wet-ice bath. A known quantity of [2-^{13}C]glycine was added as an internal concentration standard. The tissue was ground with ice-cold ethanol (1:6 wt/vol) until no visible pieces remained and the resulting homogenate was clarified by centrifugation. The supernatant was lyophilized, and resuspended in 500 μL of a phosphate-buffered (100 mmol/L, pH 7) deuterium oxide (Cambridge Isotopes) solution containing 0.5 mmol/L 3-trimethylsilyl[2,2,3,3-D_4]-propionate (TSP) as a chemical shift reference.

NMR Analysis of Cortical Extracts

Fully relaxed high-resolution ^{1}H-[^{13}C]-NMR spectra of extracts were acquired at 11.7 T. The concentrations of metabolites were determined relative to the [2-^{13}C]glycine. The isotopic ^{13}C enrichments of glutamate and glutamine were calculated from the ratio of the areas of corresponding resonances in the ^{1}H-[^{13}C]-NMR difference spectrum (^{13}C only) with the nonedited spectrum (^{12}C + ^{13}C).

Metabolic Fitting and Statistics

A two-compartment metabolic model, used for the analysis of ^{13}C turnover of glutamate and glutamine from [1-^{13}C]glucose (Gruetter *et al*, 2001; Sibson *et al*, 2001), was extended for modeling glutamate-C4 and glutamine-C4 labeling from

[2-^{13}C]acetate-Na$^+$. A two-compartment simulation of brain acetate consumption (Figure 1) was generated using CWave software, creating the group of equations listed in Table 1. The differential equations were solved using a first/second-order Runge–Kutta algorithm with plasma acetate and glucose as input functions. The fitted data consisted of the six time courses of glutamate-C4 and glutamine-C4 labeling (Group 1), the steady-state glutamine-C4 labeling from an additional 15 rats (Group 2), in which a broad range of plasma acetate concentrations were produced to allow evaluation of saturability of acetate transport and utilization, and the extract-based time courses of glutamate- and glutamine-C3 and -C4 labeling (Group 3). Specifically, ^{13}C time courses for each rat in Group 1 were fitted simultaneously with the data in Groups 2 and 3, together allowing estimates of the metabolic rates, the acetate distribution space ($V\mathrm{d}_{ac}$), and apparent values of the kinetic parameters for acetate transport (K_t, T_{max}) and consumption (K_{M_util}, V_{max_util}). The time courses of total glutamate and glutamine levels were used in the modeling. During fitting the data acquired *ex vivo* and *in vivo* were given equal weight. The *ex vivo* data had greater sensitivity, but the measurements *in vivo* contained the time-dependent information.

The introduction of acetate utilization led to the evaluation of two extremes. In the case presented in detail here, acetate is assumed to replace pyruvate, so that during the infusion, the rate of the TCA cycle in the astrocyte remains constant. The other extreme, also evaluated, is that acetate consumption was added to the flow through pyruvate dehydrogenase, leading to a time-varying astrocytic TCA cycle rate. The differences caused by the two extremes were negligible and are discussed in each section of 'Results.'

Data fitting was performed in CWave using simulated annealing hybridized with a Levenberg–Marquardt algorithm (Alcolea *et al*, 1999). Estimates of the uncertainties in the fitted parameter and their distributions were determined using a Monte Carlo analysis previously described for ^{13}C MRS studies (Mason *et al*, 1992), inspired originally from positron emission tomography (Ling and Tolhurst, 1983). The values of the function calculated at each time point for the least-squares fit were taken as an ideal, noiseless set of data, and the standard deviation of the scatter about the least-squares fit was calculated for each time course. Random Gaussian noise was added to each time course repeatedly to generate 50 simulated noisy sets of data, and the data sets were fitted with the model to generate a list of 50 values for each parameter. These values were used to estimate the distributions of uncertainty of each parameter. The significance of effects of $V\mathrm{d}_{ac}$ on the quality of the fit was evaluated by one-way ANOVA to compare the goodness of fit for each data set at different values of $V\mathrm{d}_{ac}$. Results from sensitivity analyses were compared with two-tailed *t*-tests.

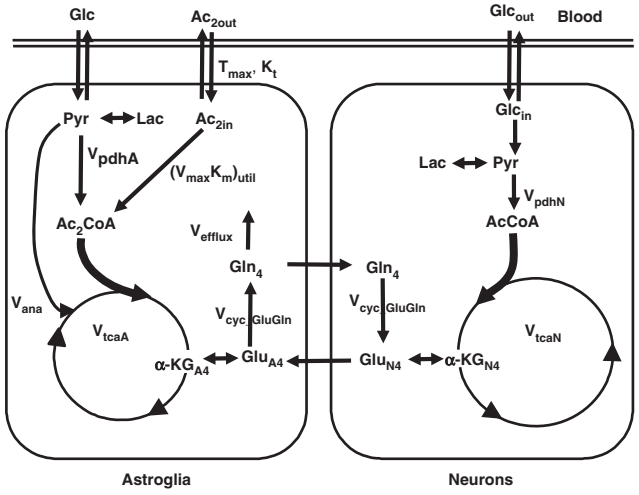

Figure 1 Two-compartment metabolic model of brain acetate transport and utilization, with pools and rates defined in Table 1. The major metabolic pathways involved in the metabolism of [2-^{13}C]acetate in brain are shown. After transport from blood to brain, [2-^{13}C]acetate is taken into astrocytes and converted to [2-^{13}C]acetyl-CoA in an ATP-dependent reaction with acetyl-CoA synthetase, generating adenosine monophosphate and inorganic phosphate as coproducts. Acetyl-CoA condenses with oxaloacetate to form citrate and subsequently α-ketoglutarate. ^{13}C label exchange between α-ketoglutarate-C4 and the small, astrocytic pool of glutamate-C4 (glutamate formation involves both transamination and reductive amination of α-ketoglutarate) leads to labeling of glutamine-C4. The flow of ^{13}C-labeled glutamine-C4 from astrocytes to neurons results in the labeling of glutamate-C4 (and GABA-C2) in neurons through the glutamate/glutamine (and GABA/glutamine) cycle.

Results

Plasma and Brain Acetate Levels During [2-^{13}C]Acetate-Na$^+$ Infusion

The baseline plasma acetate level before infusion was 0.23 ± 0.07 mmol/L. Intravenous infusion of [2-^{13}C]acetate-Na$^+$ led to a rapid increase in plasma acetate concentration and percentage enrichment ($\sim$16 mmol/L, $\sim$94%) in less than 5 min, which remained constant over the 2 h measurements (Table 2), whereas plasma glucose-C1 enrichment rose gradually to $3.5\% \pm 0.4\%$ and $4.0\% \pm 1.2\%$ by 60 and 120 min, respectively. It is assumed that glucose-C2, -C5, and -C6 were similarly labeled (Serres *et al*, 2007). A typical ^{1}H NMR spectrum from the spatially localized volume is shown in Figure 2A. The right panel of Figure 2A, which depicts individual ^{1}H NMR difference spectra with the baseline, showed brain acetate to be visible within the first 3 to 6 min of infusion. The behavior of brain acetate levels with time was similar to that of plasma acetate: after a slight lag, brain acetate increased rapidly and reached a plateau within 10 to 15 min. A graph of steady-state brain acetate levels as a function of plasma acetate level is shown in the Supplementary Material.

Metabolism of Acetate in the Brain

Figure 2B depicts representative ^{1}H-[^{13}C]-NMR spectra of the time courses of cerebral glutamine and glutamate ^{13}C labeling during the infusion of [2-^{13}C]acetate-Na$^+$ and glucose, with ^{13}C label first

Table 1 Parameters and equations used for simulation of acetate transport and consumption

Mass balance

$$\frac{dAc_{in}}{dt} = V_{acin} - (V_{acout} + V_{ac})$$

$$\frac{dGlu_N}{dt} = V_{cycle\_GluGln} + V_{xN\_KGGlu} - (V_{cycle\_GluGln} + V_{xN\_GluKG})$$

$$\frac{dGlu_A}{dt} = V_{xA\_KGGlu} + V_{cycle\_GluGln} - (V_{gln} + V_{xA\_GluKG})$$

$$\frac{dGln}{dt} = V_{gln} - (V_{cycle\_GluGln} + V_{efflux})$$

$$\frac{dKG_A}{dt} = V_{ac} + V_{xA\_KGGlu} + V_{pdhA} - (V_{xA\_KGGlu} + V_{tca\_KG})$$

$$\frac{dKG_N}{dt} = V_{tcaN} + V_{xN\_GluKG} - (V_{tcaN} + V_{xN\_KGGlu})$$

Isotope balance

$$\frac{dAc_{2in}}{dt} = V_{acin}\left(\frac{Ac_{2out}}{Ac_{out}}\right) - (V_{acout} + V_{ac})\left(\frac{Ac_{2in}}{AC_{in}}\right)$$

$$\frac{dGlu_{N4}}{dt} = V_{cycle\_GluGln}\left(\frac{Gln_4}{Gln}\right) + V_{xN\_KGGlu}\left(\frac{KG_{N4}}{KG_N}\right) - (V_{cycle\_GluGln} + V_{xN\_GluKG})\left(\frac{Glu_{N4}}{Glu_N}\right)$$

$$\frac{dGlu_{N3}}{dt} = V_{cycle\_GluGln}\left(\frac{Gln_3}{Gln}\right) + V_{xN\_KGGlu}\left(\frac{KG_{N3}}{KG_N}\right) - (V_{cycle\_GluGln} + V_{xN\_GluKG})\left(\frac{Glu_{N3}}{Glu_N}\right)$$

$$\frac{dGlu_{A4}}{dt} = V_{xA\_KGGlu}\left(\frac{KG_{A4}}{KG_A}\right) + V_{cycle\_GluGln}\left(\frac{Glu_{N4}}{Glu_N}\right) - (V_{gln} + V_{xA\_GluKG})\left(\frac{Glu_{A4}}{Glu_A}\right)$$

$$\frac{dGlu_{A3}}{dt} = V_{xA\_KGGlu}\left(\frac{KG_{A3}}{KG_A}\right) + V_{cycle\_Glugln}\left(\frac{Glu_{N3}}{Glu_N}\right) - (V_{gln} + V_{xA\_GluKG})\left(\frac{Glu_{A3}}{Glu_A}\right)$$

$$\frac{dGln_4}{dt} = V_{gln}\left(\frac{Glu_{A4}}{Glu_A}\right) - (V_{cycle\_GluGln} + V_{efflux})\left(\frac{Gln_4}{Gln}\right)$$

$$\frac{dGln_3}{dt} = V_{gln}\left(\frac{Glu_{A3}}{Glu_A}\right) - (V_{cycle\_GluGln} + V_{efflux})\left(\frac{Gln_3}{Gln}\right)$$

$$\frac{dKG_{A4}}{dt} = V_{ac}\left(\frac{Ac_{2in}}{Ac_{in}}\right) + V_{xA\_KGGlu}\left(\frac{Glu_{A4}}{Glu_A}\right) + \frac{1}{2}V_{pdhA}\left(\frac{Glc_1+Glc_6}{Glc}\right) - (V_{xA\_KGGlu} + V_{tca\_kg})\left(\frac{KG_{A4}}{KG_A}\right)$$

$$\frac{dKG_{A3}}{dt} = V_{xA\_GluKG}\left(\frac{Glu_{A3}}{Glu_A}\right) + \frac{1}{2}V_{tcA\_KG}\left(\frac{KG_{A4}}{KG_A}\right) + \frac{1}{2}V_{tcA\_KG}\left(\frac{KG_{A3}}{KG_A}\right) + \frac{1}{4}V_{ana}\left(\frac{Glc_1+Glc_2+Glc_5+Glc_6}{Glc}\right) - (V_{xA\_KGGlu} + V_{tca\_KG})\left(\frac{KG_{A3}}{KG_A}\right)$$

$$\frac{dKG_{N4}}{dt} = \frac{1}{2}V_{pdhN}\left(\frac{Glc_1+Glc_6}{Glc}\right) + V_{xN\_GluKG}\left(\frac{Glu_{N4}}{Glu_N}\right) - (V_{tcaN} + V_{xN\_KGGlu})\left(\frac{KG_{N4}}{KG_N}\right)$$

$$\frac{dKG_{N3}}{dt} = V_{xN\_GluKG}\left(\frac{Glu_{N3}}{Glu_N}\right) + \frac{1}{2}V_{tcaN}\left(\frac{KG_{N4}}{KG_N}\right) + \frac{1}{2}V_{tcaN}\left(\frac{KG_{N3}}{KG_N}\right) - (V_{tcaN} + V_{xN\_KGGlu})\left(\frac{KG_{N3}}{KG_N}\right)$$

Combination pools

$Glu_{4\_total} = Glu_{A4} + Glu_{N4}$
$Glu_{3\_total} = Glu_{A3} + Glu_{N3}$

Rates

$\boldsymbol{K_{M_util}} = 0.17\ \mu$mol/g ($K_M$ for acetate consumption)

$\boldsymbol{K_t} = 26.9$ mmol/L (K_M for blood–brain import of acetate, called K_t in the text)

Table 1 *Continued*

$\boldsymbol{T_{max}} = 2.1\ \mu$mol/min/g ($V_{max}$ for blood–brain transport of acetate)

$V_{ac} = V_{max\_util} * Ac_{in}/Vd_{ac}/(K_{M\_util}+Ac_{in}/Vd_{ac})$ (rate of acetate consumption, initial value = 0.01 μmol/min/g)

$V_{ac\_in} = T_{max} * Ac_{out} * Vd_{ac}/(Ac_{out} * Vd_{ac}+Ac_{in}+K_t * Vd_{ac})$ (rate of acetate import, initial value = 0.011 μmol/min/g)

$V_{ac\_out} = T_{max} * Ac_{in}/(Ac_{out} * Vd_{ac}+Ac_{in}+K_t * Vd_{ac})$ (rate of acetate export, initial value = 0.001 μmol/min/g)

$V_{ana} = 0.2 * V_{gln} = 0.114\ \mu$mol/min/g (rate of anaplerosis; Sibson *et al*, 2001)

$V_{cycle_GluGln} = V_{gln}+V_{xA_GluKG}-V_{xA_KGGlu}+V_{netGlu} = 0.48\ \mu$mol/min/g (rate of glutamate–glutamine cycling)

$\boldsymbol{Vd_{ac}} = 0.32$ mL/g (brain acetate distribution space)

$V_{efflux} = V_{ana}-V_{netGlu}-V_{netGln} = 0.0967\ \mu$mol/min/g (rate of loss of carbon from astrocytic TCA cycle through Glu_A and Gln)

$\boldsymbol{V_{gln}} = 0.57\ \mu$mol/min/g (rate of glutamine synthesis)

$\boldsymbol{V_{max_util}} = 0.14\ \mu$mol/min/g ($V_{max}$ of acetate consumption)

$\boldsymbol{V_{netGln}} = 0.0167\ \mu$mol/min/g (rate of increase of glutamine from the system, based on time-dependent measurements of glutamine concentration changes)

$\boldsymbol{V_{netGlu}} = 0.0206\ \mu$mol/min/g (rate of increase in glutamate from the system, based on time-dependent measurements of glutamate concentration changes)

$V_{pdhA} = V_{tcaA}-V_{ac} = 0.33\ \mu$mol/min/g (astrocytic pyruvate dehydrogenase rate)

$\boldsymbol{V_{pdhN}} = V_{tcaN} = 1.41\ \mu$mol/min/g (neuronal pyruvate dehydrogenase rate)

$\boldsymbol{V_{tcaA}} = 0.37\ \mu$mol/min/g (astrocytic TCA cycle rate)

$V_{tcaA_KG} = V_{tcaA}-V_{ana} = 0.26\ \mu$mol/min/g (astrocytic TCA cycle rate following α-ketoglutarate)

$\boldsymbol{V_{tcaN}} = 1.41\ \mu$mol/min/g (neuronal TCA cycle rate)

$\boldsymbol{V_{xA\_GluKG}} \geqslant V_{tcaA}$ (rate of flow from Glu_A to KG_A; value indeterminate)

$V_{xA_KGGlu} = V_{xA_GluKG}+V_{ana}\ \mu$mol/min/g (rate of flow from KG_A to Glu_A; value indeterminate)

$\boldsymbol{V_{xN_GluKG}} = 89\ \mu$mol/min/g (rate of flow from Glu_N to KG_N)

$V_{xN_KGGlu} = V_{xN_GluKG} = 89\ \mu$mol/min/g (rate of flow from KG_N to Glu_N)

Pool concentrations

$Ac_{in} = 0.01\ \mu$mol/g (preinfusion level of brain acetate; immeasurably small, estimated from fitted kinetics)

$fGlu_A = 0.015$ (fraction of astrocytic glutamate)

Gln = 6 μmol/g at baseline (brain glutamine; measured over time)

$Glu_A = fGlu_A * Glu_{Total}$ (astrocytic glutamate, 0.14 μmol/g at baseline)

$Glu_N = Glu_{Total}-Glu_A$ (neuronal glutamate, 9.26 μmol/g)

$Glu_{Total} = 9.4\ \mu$mol/g at baseline (brain glutamate; measured over time)

$KG_A = 0.02\ \mu$mol/g (astrocytic α-ketoglutarate)

$KG_N = KG_{Total}-KG_A = 0.2\ \mu$mol/g (neuronal α-ketoglutarate)

$KG_{Total} = 0.22\ \mu$mol/g (total α-ketoglutarate; Hawkins and Mans (1983)

Parameters whose values were determined iteratively are shown in bold-faced type.

Table 2 Systemic physiological parameters, plasma metabolite levels, and ^{13}C enrichments during intravenous [2-^{13}C]acetate-Na^+ infusion

Parameters	*Time (min)*							
	0	*1*	*3*	*5*	*10*	*25*	*55*	*120*
pH	7.24 ± 0.10	—	—	7.31 ± 0.07	—	7.39 ± 0.10	3.37 ± 0.08	7.47 ± 0.09
pCO_2 (mHg)	37 ± 10	—	—	44 ± 14	—	36 ± 9	53 ± 26	46 ± 2
pO_2 (mHg)	154 ± 23	—	—	144 ± 28	—	130 ± 16	131 ± 54	133 ± 48
[Acetate] (mmol/L)	0.2 ± 0.1	1.6 ± 1.3	10.9 ± 3.0	19.4 ± 5.0	17.0 ± 2.3	17.7 ± 2.2	15.8 ± 3.0	17.6 ± 0.4
[2-^{13}CAcetate] (%)[a]	0	42 ± 46	94 ± 1	96 ± 4	93 ± 2	91 ± 1	90 ± 2	90 ± 2
[Lactate] (mmol/L)	0.54 ± 0.28	0.82 ± 0.22	0.83 ± 0.29	0.75 ± 0.20	0.62 ± 0.17	0.97 ± 0.32	0.83 ± 0.24	—
[Alanine] (mmol/L)	0.27 ± 0.17	0.32 ± 0.15	0.34 ± 0.16	0.28 ± 0.11	0.26 ± 0.08	0.27 ± 0.08	0.13 ± 0.09	—

[2-^{13}C]acetate-Na^+ was infused using a bolus-variable rate infusion at 1.25 mmol/min/kg (0 to 5 min), 0.625 mmol/min/kg (5 to 10 min), and 0.25 mmol/min/kg thereafter until the end of the experiment. Acetate concentrations and enrichments were measured with ^1H NMR as described in 'Materials and methods.'
[a]Percentage enrichments reflect excess above natural abundance of 1.1%. Values represent mean ± s.d.

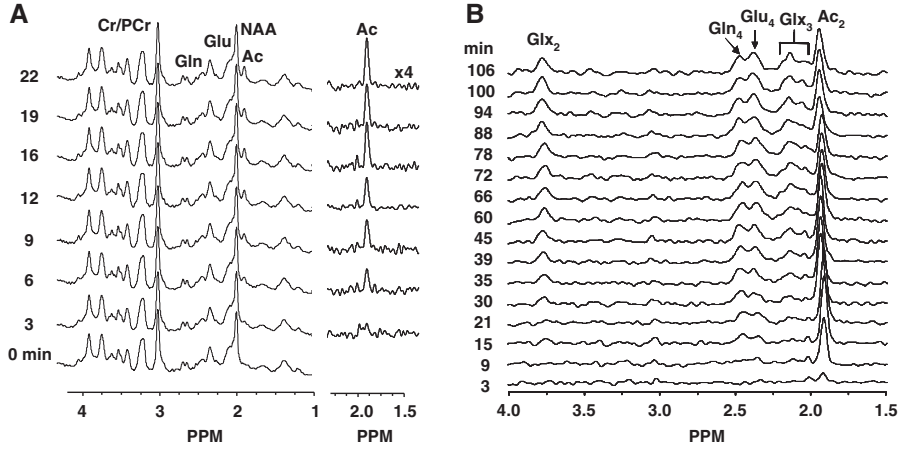

Figure 2 (**A**) Spatially localized ^{1}H-[^{13}C]-NMR spectra of the brain of an anesthetized rat during the infusion of [2-^{13}C]acetate-Na^{+}. A spectrum acquired before acetate-Na^{+} infusion was subtracted from each spectrum acquired during infusion to better reveal the brain acetate signal (right panel). The rise in the brain acetate signal (singlet, 1.9 p.p.m.) could be seen clearly by 6 min of infusion. (**B**) Representative time courses of ^{13}C labeling of cerebral metabolites from [2-^{13}C]acetate-Na^{+}. The midpoint time of spectrum acquisition is depicted to the left of each spectrum. The ^{1}H-[^{13}C]-NMR difference spectrum was obtained by subtracting the ^{13}C-inverted (^{12}C$-^{13}$C) spectrum from the noninverted (^{12}C + ^{13}C) spectrum leaving only the ^{13}C-coupled ^{1}H resonances, at a relative intensity of $2 \times {}^{13}$C. [2-^{13}C]acetate-Na^{+} was infused using a bolus-variable rate infusion at 1.25 mmol/min/kg (0 to 5 min), 0.625 mmol/min/kg (5 to 10 min), and 0.25 mmol/min/kg (final) thereafter until the end of the experiment. The protocol maintained plasma acetate concentration and percent ^{13}C enrichment at $\sim$18 mmol/L and over 90%, respectively, throughout the experiment. Peak label definitions: Ac, acetate; Cr, creatine; Gln, glutamine; Glu, glutamate; NAA, *N*-acetylaspartate; PCr, phosphocreatine, Ac_2, acetate-C2; Gln_4, glutamine-C4; Glu_4, glutamate-C4; Glx_2, (glutamate-C2 + glutamine-C2); Glx_3, (glutamate-C3 + glutamine-C3). Spectra were recorded from a volume of $\sim$196 μL ($7 \times 4 \times 7$ mm^3).

appearing in glutamine-C4 (Figure 3C) followed by glutamate-C4 (Figures 3D and 3F). This pattern is consistent with the astrocytic localization of acetate metabolism and glutamine synthesis followed by glutamate replenishment in neurons through the glutamate/glutamine cycle. This is in contrast to the labeling pattern observed with [1,6-$^{13}C_2$]glucose, in which label appears first in glutamate-C4 and followed by glutamine-C4. Late in the infusion, the glutamate-C4 peak becomes larger, but because glutamate has a much greater concentration, its percent enrichment remains much lower than that of glutamine-C4, which is reflective of astrocytic consumption of acetate.

Glutamate and glutamine concentrations increased slowly with time during the [2-^{13}C]acetate-Na^{+} infusion, with rates of 0.021 and 0.017 μmol/g/min, respectively, as has been reported previously in mice infused with acetate-Na^{+} (Chowdhury *et al*, 2007). In the present analysis, the increases in glutamate and glutamine were accommodated in the model through increased astrocytic anaplerosis, which provided the additional mass. Their increased levels may reflect an osmotic effect of an increased plasma sodium load as discussed below.

To assess whether acetate utilization is limited at the level of transport or metabolism, or some combination of both, the steady-state ^{13}C labeling of glutamine-C4, measured after 40 min of [2-^{13}C]acetate-Na^{+} infusion, was evaluated at different plasma acetate levels. For steady-state measurements, 40 min time was chosen because under our experimental conditions, namely infusion of [2-^{13}C]acetate-Na^{+} and glucose under halothane, glutamine-C4 labeling has reached its plateau by this time (Figures 3C and 3F). Analysis of the steady-state glutamine-C4 labeling in relation to increasing plasma acetate concentrations indicated that acetate oxidation in the astrocytic TCA cycle reached 90% saturation for plasma acetate concentrations of 7 mmol/L (Figure 3B). This indicates that at high blood acetate levels, brain acetate utilization is capped by saturation of metabolism (enzyme activity) and not by transport, whereas the initial lag results from delays incurred by transport and metabolism, similar to what was reported recently (Deelchand *et al*, 2009*b*). In that study, 90% saturation of acetate consumption was estimated to occur at 6 mmol/L, similar to what was seen in this study. As the time courses of glutamine-C4 labeling were similar for such high values of plasma acetate, any slight shortfall from steady state will be uniformly underestimated for all plasma values and therefore yield saturation at about the same level. That is, a slight underestimation of the steady-state glutamine-C4 labeling will be uniform and have a negligible impact on the value of plasma acetate observed to saturate acetate metabolism.

The infusion of [2-^{13}C]acetate-Na^{+} led to some ^{13}C labeling of plasma glucose-C1, presumably reflecting metabolism of the acetate by the liver. Although we did not measure the other glucose carbon atom positions, Serres *et al* (2007) reported

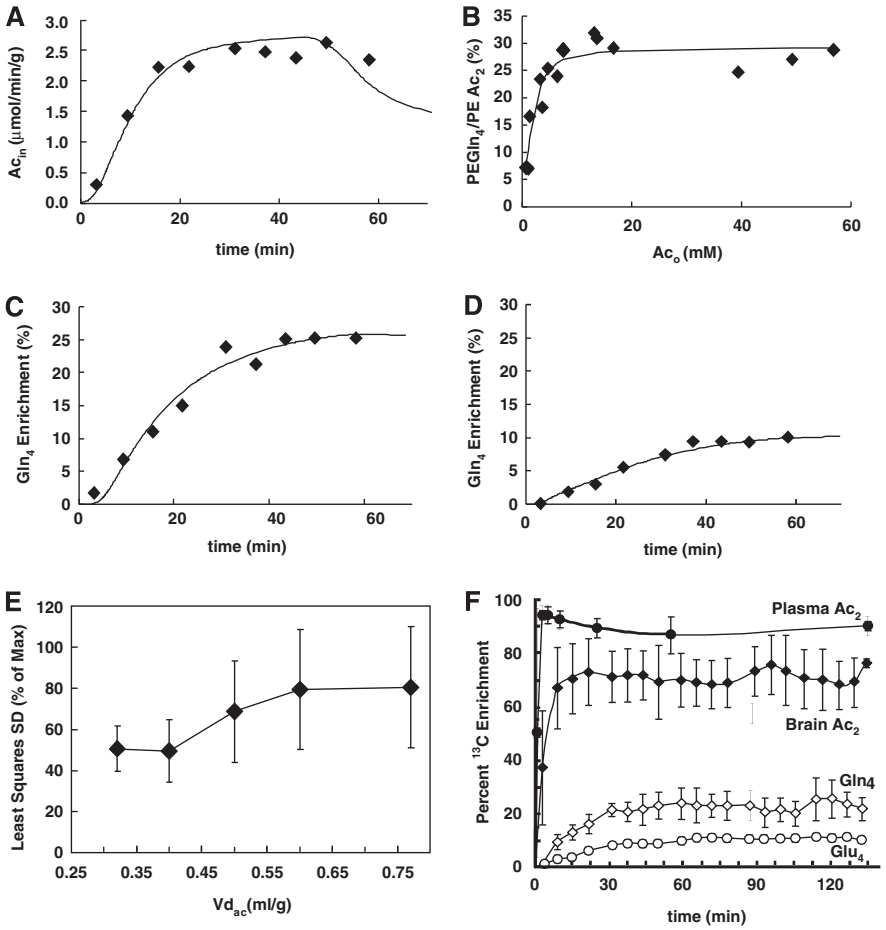

Figure 3 Fit of metabolic model to measured data. (**A**) Brain acetate level with time in one animal, (**B**) steady-state glutamine-C4 enrichment for all the animals measured at 40 min after [2-^{13}C]acetate-Na$^+$ infusion at a range of concentrations of plasma acetate, with the ratio percent enrichment (PE) glutamine-C4/PE acetate-C2 calculated as the ratio of the percent ^{13}C enrichment of glutamine-C4 with plasma acetate-C2 and multiplied by 100. The final acetate-Na$^+$ infusion rates to achieve plasma acetate levels were 0.05, 0.10, 0.15, 0.25, and 0.50 mmol/kg/min. (**C**) Glutamine-C4 and (**D**) glutamate-C4 turnover as functions of time after the start of the infusion of [2-^{13}C]acetate-Na$^+$ in the same animal as shown in (**A**). Lines represent the best fit of metabolic model to measured data. (**E**) Variation of least squares s.d. with brain acetate distribution space. (**F**) Averaged data showing ^{13}C labeling of plasma and brain acetate, and ^{13}C turnover of glutamine-C4 (Gln4) and glutamate-C4 (Glu4). The final acetate-Na$^+$ infusion rate was 0.25 mmol/kg/min in (**A**), (**C**), (**D**), (**E**), and (**F**), and the acetate levels and [2-^{13}C] enrichments averaged 17 mmol/L and 90%, respectively, during the infusions.

that plasma glucose C1, C2, C5, and C6 are labeled similarly, and this label pattern was assumed in this study and included in the analysis. Metabolism of glucose labeled at C1 and C6 leads to pyruvate labeled at C3, whereas glucose labeled at C2 and C5 produces pyruvate labeled at C2. Anaplerosis was assumed to carry label from pyruvate C3 to oxaloacetate C3 and, hence, to glutamate/glutamine-C2, and from pyruvate C2 to oxaloacetate C2 and, hence, glutamate/glutamine-C3. Backward flow of the ^{13}C label between oxaloacetate and fumarate in the astrocytic TCA cycle will scramble the ^{13}C label in oxaloacetate at C2 and C3. This process will cause half the anaplerosis-derived label from pyruvate C3 to appear at the C3 of glutamate/glutamine and half the anaplerosis-derived label from pyruvate C2 to appear at the C2 of glutamate/glutamine; the equation for astrocytic α-ketoglutarate-C3 in Table 1 expresses that scenario. If gluconeogenesis in the blood labels the C1, C2, C5, and C6 of glucose similarly (Serres *et al*, 2007), then scrambling between oxaloacetate C2 and C3 will not change the distribution of ^{13}C label, and the equation for α-ketoglutarate given in Table 1 will yield the same result. However, should label scrambling not occur, the astrocytic α-ketoglutarate-C3 will retain all its anaplerotically derived label from pyruvate-C2 but obtain none from pyruvate-C3, and the value of the term for V_{ana} will remain the same.

The value of V_{xA} was indeterminate, subject only to the constraint that $V_{xA} \geqslant V_{tcaA.}$ A sensitivity analysis showed that for the five rats that were fitted individually, whether $V_{xA} = V_{tcaA}$ or $V_{xA} \gg V_{tcaA}$, the difference in the overall goodness of fit was insig-

nificant ($P = 0.46$). There were no significant differences in any of the fitted parameters (the most significant P-value was 0.22).

Transport Kinetics and Utilization of Acetate in the Brain

Michaelis–Menten constants for transport and metabolism of acetate, as well as the acetate distribution space, were calculated by fitting a two-compartment metabolic model shown in Figure 1 and Table 1 to the ^{13}C turnover curves of glutamine-C4, glutamate-C4, acetate-C2, and steady-state glutamine-C4 labeling (Figures 3A to 3D). In this model, acetate transport and metabolism were assumed to follow reversible symmetric Michaelis–Menten kinetics. On the basis of this model, K_t and T_{max} for transport were 27 ± 2 mmol/L and 1.3 ± 0.3 μmol/g/min, respectively, with a brain distribution space for acetate of 0.32 ± 0.12 mL/g. In contrast, the K_{M_util} and V_{max_util} for acetate utilization were 0.17 ± 0.24 mmol/L and 0.14 ± 0.02 μmol/g/min, respectively, although without making measurements at lower values of acetate, it is more conservative to say that K_{M_util} is much lower than the concentrations used in this study.

The slow acetate transport led to a 5-min delay for brain acetate to reach 50% of its steady-state concentration and 3 to 5 min for acetate oxidation to reach 95% of its steady-state rate. The estimated neuronal TCA cycle and glutamine synthesis rates were 1.41 ± 0.11 and 0.57 ± 0.08 μmol/g/min, respectively. The astrocytic TCA cycle flux was 0.35 ± 0.05 μmol/g/min, which is $21\% \pm 3\%$ of the total (neuronal + astrocytic) TCA cycle rate. The relative enrichments of glutamate-C4, glutamine-C4, and acetate-C2 also showed that under saturating conditions, acetate supplied carbon for $41\% \pm 11\%$ of the astrocytic TCA cycle rate.

If V_{tcaA} was allowed to rise with V_{ac} added to V_{pdhA}, then no parameters changed significantly (most significant $P = 0.13$). The distribution space was negligibly affected by the treatment of V_{tcaA}, changing to 0.33 mL/g. The neuronal and baseline astrocytic TCA cycle rates also changed negligibly, to 1.26 and 0.34 μmol/g/min, respectively ($P = 0.38$ and 0.43, respectively).

Assuming only carrier-mediated transport of acetate (coefficient of diffusion $K_d = 0$), we found K_t to be 21 mmol/L. When a purely diffusive coefficient is used, which carries with it the inherent assumption that acetate is distributed throughout the brain water space, it was possible to obtain fits that were compatible with either the steady state or the kinetic portions of the data, but not both. When a diffusive component was included as an *additional* transport mechanism, the apparent K_t for transport was lower, 10 mmol/L, which is nearer the values reported for cultured astrocytes and calculated from the brain uptake index (BUI) for acetate.

Distribution Space of Acetate in Brain

The acetate transport constants in this study were estimated by an analysis of the steady-state brain and blood acetate concentrations when fitted to a symmetric, reversible Michaelis–Menten transport model with saturable consumption, in analogy to a previous study of glucose transport (de Graaf *et al*, 2001). In this case, the distribution space was considered to be the volume to which acetate has access. The sensitivity of the data and analysis to the acetate distribution space were tested by fitting the data with Vd_{ac} fixed at values ranging from the estimated value of 0.32 mL/g to the full brain water space of 0.77 mL/g (Buschiazzo *et al*, 1970; Gjedde and Diemer, 1983), with the best fit at 0.32 mL/g, which repeated-measures ANOVA showed to have a significant effect on the ($F(4,20) = 4.22$, $P = 0.012$).

In a recent study, Deelchand *et al* (2009*b*) addressed the transport and utilization of [2-^{13}C]acetate-Na^+ in anesthetized rats while reporting time courses of brain acetate and labeling of glutamate and glutamine. Although the time courses appear similar to those in this study, the kinetic constants for blood–brain acetate transport differ from the present results. In their study, a brain distribution space of 0.77 mL/g was assumed for acetate, and the kinetic analysis considered only the brain acetate but not the observed incorporation of ^{13}C into glutamate and glutamine. These factors are likely to explain the different kinetic constants obtained. Indeed, when glutamate and glutamine labeling was ignored, we were able to use a wide range of values for Vd_{ac} to fit the brain acetate. For a value equal to the brain water space of 0.77 mL/g, we found values of 4.1 mmol/L and 0.8 μmol/g/min for K_t and T_{max}, similar to the 4.2 and 0.96 in the recent report (Deelchand *et al*, 2009*b*). We also found that with $Vd_{ac} = 0.77$ mL/g, K_{M_util} was low (< 0.5 mmol/L), and V_{max_util} was 0.46 μmol/g/min, also similar to the values of 0.02 mmol/L and 0.53 μmol/g/min reported in the previous study.

Distributions of the Fitted Parameters

The uncertainties in the fitted parameters from ^{13}C turnover data were estimated by Monte Carlo analysis (Figure 4). The uncertainty distributions were generally symmetrical, indicating that the means of the parameter estimates are representative of the expected values, that the standard deviations accurately describe the distributions, and that parameter estimates were well determined.

Discussion

In this study, we accessed the rates of transport and utilization of acetate in cortex of anesthetized rats by analysis of ^{13}C steady-state enrichments and dynamic ^{13}C turnover curves for glutamine-C4 and

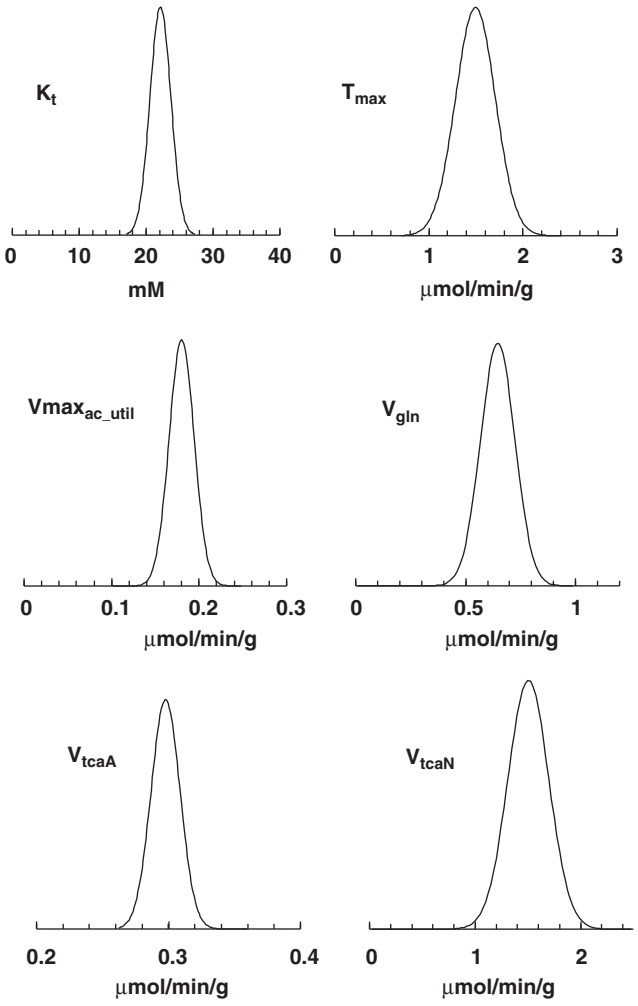

Figure 4 Distributions of parameters in a representative set of data (Ling and Tolhurst, 1983; Mason *et al*, 1992). The graphs represent the variation in transport parameters and cerebral metabolic fluxes derived from the ^{13}C turnover of glutamine-C4 and glutamate-C4 obtained from one rat. The uncertainty distributions were generally symmetrical, indicating that the means of the parameter estimates are representative of the expected values, that the standard deviations accurately describe the distributions, and that parameter estimates were well determined.

glutamate-C4 during [2-^{13}C]acetate-Na^+ infusion. To extract the relevant kinetic information from the NMR data, we extended a two-compartment (neuron-astrocyte) metabolic model used in analyses of labeling from [1-^{13}C]glucose (Gruetter *et al*, 2001; Sibson *et al*, 2001) to include separate steps for acetate transport and utilization (Figure 1; Table 1). The rate of acetate utilization (V_{ac}) increased with blood acetate concentration, reaching saturation for $[Ac]_{plasma} > 15$ mmol/L. Consequently, acetate utilization as a percentage of total astrocytic oxidation increased from $\sim$13% at basal blood acetate levels (0.23 mmol/L) to >40% when blood acetate was at saturating levels. The distribution space for acetate (Vd_{ac}) of 0.32 ± 0.12 mL/g in the measured cortical volume was found to be much less than the value for glucose, which was the total brain water space of 0.77 mL/g (Buschiazzo *et al*, 1970; Gjedde and Diemer, 1983), indicating that acetate was not accessible to all brain/cellular compartment(s). Our findings support recent studies of the quantitative extent of astrocytic acetate oxidation (Cruz *et al*, 2005; Hertz, 2004), but emphasize the dependence on plasma concentration and saturability of acetate utilization *in vivo*.

Brain Acetate Transport and the Acetate Distribution Space

Transport of acetate from blood to brain involves both carrier-mediated cotransport of the anion with a hydrogen ion and diffusion of acetic acid (Halestrap *et al*, 1997). Under physiologic conditions of pH and low blood concentrations (<1 mmol/L), carrier-mediated transport of acetate is believed to be dominant (Terasaki *et al*, 1991), involving H^+-coupled monocarboxylate transporters (MCTs), as for the other physiologically common monocarboxylates (e.g., lactate, pyruvate, 3-hydroxybutryate, acetoacetate). Of the seven known members of the MCT family, three are found in brain (MCT1, MCT2, and MCT4), with each having cell-type-specific patterns of expression and different transport properties. Although MCT1 is expressed on capillary endothelium and ventricular ependymal cells, as well as astrocytes, MCT2 is expressed in neurons, whereas MCT4 is exclusively astrocytic (Bergersen *et al*, 2002; Gerhart *et al*, 1997). As noted previously (Waniewski and Martin, 1998), the different MCT isoforms on astrocytes and neurons may account for the capacity of astrocytes to use acetate, because acetyl-CoA synthetase, the enzyme that activates acetate to acetyl-CoA, is expressed at comparable levels in both cell types. Exclusion of acetate from neurons could account for the low value of the acetate distribution space (Vd_{ac}) that we found in this study.

In contrast to the other monocarboxylates in which transport parameters (K_t, T_{max}) are reasonably well characterized, far less information is available for brain acetate transport for comparison with this study. An Eadie–Hofstee plot of BUI data for acetate reported earlier (Oldendorf, 1973) yields an apparent K_t of 6.7 mmol/L (The K_M for acetate transport was estimated from published data (Oldendorf, 1973). BUI data were corrected for passive (diffusive) transport determined for sucrose (2.9%; Gjedde and Crone, 1975) to give the facilitated component, BUI_f. K_M was calculated from the slope ($-K_M$) of a plot of BUI_f versus $BUI_f/[C_a]$ (Eadie–Hofstee), where $[C_a]$ is the arterial acetate concentration.). In bovine capillary endothelial cell prepared as monolayers, K_t was 3.41 mmol/L, and as isolated cells, 2.22 mmol/L (Terasaki *et al*, 1991). Those values are comparable to K_ts reported for blood–brain-barrier transport of lactate 1.9 to 3.8 mmol/L (Gjedde and Crone, 1975; Kuhr *et al*, 1988; Pardridge and Oldendorf, 1977). In

cultured astrocytes, the transport K_t for acetate was 9.3 ± 5.0 mmol/L (Waniewski and Martin, 1998). As noted above, astrocytes express both MCT1 and MCT4, so the apparent K_t is expected to be a weighted average of their respective affinities and cell-surface densities. The affinity of MCT4 for monocarboxylates is an order of magnitude or more lower than MCT1 (Dimmer *et al*, 2000; Manning Fox *et al*, 2000); for acetate K_t >100 mmol/L (Dimmer *et al*, 2000). Thus, the intermediate values seen for astrocytes may reflect a mixture of these two transporters. However, the possible participation of other transport carriers for acetate cannot be excluded (Waniewski and Martin, 1998).

The observed K_t for acetate transport is an apparent K_t whose value reflects competition with other monocarboxylic acids, the most abundant of which is lactate. If the K_t for lactate transport is 1.9 to 3.8 mmol/L (Gjedde and Crone, 1975; Kuhr *et al*, 1988; Pardridge and Oldendorf, 1977), and the concentration of plasma lactate was 0.75, then the observed K_t for acetate in the presence of lactate is expected to be 15 to 17 mmol/L or, if a diffusive component is included, then 7 to 8 mmol/L.

One consequence of the transport kinetics is a delay of several minutes between administration of isotopically labeled acetate and its arrival in the brain. In this study, there was a delay of ~5 min between the introduction of the acetate-Na^+ in the blood and the time it took to achieve 95% of its final level in the brain. During this time the blood pool of ^{13}C-labeled acetate is much greater than in brain.

Of particular interest is the value of the acetate distribution space (32% ± 12%), which has not been reported earlier. Acetate is not believed to be transported into neurons, in that transport of acetate into isolated nerve terminals was shown to be minimal, with diffusion accounting for ~0.1% of the astrocytes (Waniewski and Martin, 1998). Assuming that the extracellular fluid comprises 15% of the brain water space (Baethmann *et al*, 1970), and that acetate has access to the extracellular fluid and the astrocytic compartment, then the remaining astrocytic volume in cortex would be given by the difference between 32% and 15%, or 17% ± 13% would comprise the astrocytic volume (with 1 s.d., up to 30%), similar to values reported earlier (Williams *et al*, 1980). We saw no relationship between the calculated values of the distribution space and plasma acetate levels up to 20 mmol/L ($r^2 = 0.002$). However at a higher level of acetate, than that studied here, significant diffusion of acetate into neurons may increase the value of Vd_{ac}.

Labeling of Amino Acids From Acetate

[2-^{13}C]Acetate-Na^+ is metabolized in astrocytes, labeling the small pool of glutamate that serves as precursor for glutamine synthesis (Lebon *et al*, 2002; van den Berg and Garfinkel, 1971). If acetate is the sole precursor for glutamine then at steady state the labeling of [4-^{13}C]glutamine should be equal to precursor plasma [2-^{13}C]acetate. The observed percentage labeling of glutamine-C4 (~25%) is much less than plasma [2-^{13}C]acetate (90%). The lower labeling of glutamine than acetate is mainly explained by dilution at both the acetyl-CoA level owing to pyruvate dehydrogenase (PDH) activity (in both neurons and astrocytes), and at the glutamine level owing to inflow of blood glutamine (Serres *et al*, 2008). Glucose could be used for acetate synthesis, and degradation of acetylcholine can also dilute brain acetate labeling relative to plasma. In our measurement, brain [2-^{13}C]acetate labeling (75%) is less than plasma acetate (90%), suggesting 15% to 20% dilution of brain acetate relative to plasma (Figure 3F). Furthermore, the measured ^{13}C labeling of glutamine-C4 (25%) is much lower than brain [2-^{13}]acetate (75%), leading to ~65% dilution. This suggests major flow (up to 65% to 70%) of unlabeled carbon into glutamine form glucose through glutamate–glutamine cycling. In fact, experiments conducted with [1-^{13}C]glucose/[1,6-$^{13}C_2$]glucose indicate 20% to 30% dilution of glutamine-C4 relative to its precursor glutamate-C4 (Oz *et al*, 2004) indicating a contribution of the glutamate/glutamine pathway for the repletion of glutamine of up to ~70% (Patel *et al*, 2005).

Glutamine dilution can also arise from the exchange of glutamine between blood and brain (Broer and Brookes, 2001; Serres *et al*, 2008). This mechanism of dilution was not included in the analysis because it has the same effect on glutamine labeling as the oxidation of unlabeled glucose in the astrocyte (Oz *et al*, 2004; Shen *et al*, 2009). Accordingly, when V_{dilGln} was included in the model, the quality of the fit was not affected ($P = 0.69$), and rate estimates were not significantly altered (greatest P-value = 0.21). The exchange may in fact occur but was not measurable in this study.

The Rate of Brain Acetate Utilization

Acetate is a normal component of blood, present at about 0.2 to 0.9 mmol/L in the rat under normal physiologic conditions. The minimum cerebral utilization rate of blood-borne acetate, based on tracer analysis of [2-^{14}C]acetate and autoradiography in the presence of 0.94 mmol/L plasma acetate, ranges from 0.11 to 0.14 μmol/g/min in the cortex of the awake rat, or ~15% to 25% of glucose utilization at rest (Cruz *et al*, 2005). This estimate is about 3.0 to 3.8 times higher than the value of 0.037 μmol/g/min predicted for blood acetate of 0.94 mmol/L based on the kinetics estimated in our study of rats under halothane anesthesia. Cruz *et al* (2005) reported a small increase in [2-^{14}C]acetate utilization during acoustic stimulation in awake rats, although the increase was much less than for 2-deoxy-[^{14}C]glucose, and unlike the latter was not proportional to stimulation rate. Although our lower predicted value

for cortical acetate utilization would be consistent with a suppressing effect of anesthesia on glial oxidative metabolism (Choi *et al*, 2002; Oz *et al*, 2004), further study using the same methodology is needed to confirm this.

Acetate is converted to acetyl-CoA by acetyl-CoA synthetase (AceCS, ACS; E.C. 6.2.1.1), which is expressed in astrocytes and neurons (Brand *et al*, 1997). In astrocytes and isolated nerve terminals AceCS activity is found in both cytosol and the mitochondria (Waniewski and Martin, 1998). Two AceCS isoforms are expressed in brain: AceCS1, which is present in cytosol, and AceCS2, which is present in the mitochondrial matrix (Fujino *et al*, 2001). AceCS2 may catalyze acetate oxidation, as this isoform is specifically upregulated under ketogenic conditions, whereas AceCS1 is involved in fatty acid biosynthesis (Ikeda *et al*, 2001). Both AceCS isoforms possess high affinities (low K_ts) for acetate: AceCS1, $\sim$0.11 mmol/L and AceCS2, $\sim$0.06 mmol/L (Fujino *et al*, 2001). Although the apparent K_t for acetate with respect to utilization could not be determined accurately *in vivo*, the upper limit found, $K_t < 0.25$ mmol/L, is of a comparable magnitude to the 0.14 mmol/L for AceCS studied in rat brain homogenates and the 0.28 mmol/L found with recombinant DNA expression of human AceCS (Luong *et al*, 2000). Furthermore, the rate of 0.14 μmol/g/min for acetate utilization under saturating plasma acetate levels is about one-third of the V_{max} of 0.41 μmol/g/min for AceCS measured in rat brain homogenates (Reijnierse *et al*, 1976). Thus, the present findings are compatible with AceCS limiting acetate utilization, consistent with previous studies *in vitro* and *in vivo* on the nature of this enzyme.

Comparison of Rates Determined With Infusion of [2-^{13}C]Acetate-Na$^+$ or [1-^{13}C]Glucose

The values of rates determined with [2-^{13}C]acetate for the neuronal TCA cycle (V_{tcaN}, 1.41 ± 0.11 μmol/g/min or $\sim$0.70 μmol/g/min in terms of neuronal glucose oxidation) and glutamine synthesis (V_{gln}, 0.57 ± 0.08 μmol/g/min) are similar to their values determined with [1,6-$^{13}C_2$]glucose/unlabeled acetate (neuronal oxidative glucose utilization = 0.60 μmol/g/min, $V_{gln} = 0.58$ μmol/g/min; Patel *et al*, 2005) in rats prepared similarly and anesthetized with halothane.

The astrocytic TCA cycle flux was 0.37 ± 0.03 μmol/g/min, ranging from 19% to 24% of total TCA cycle flux contributed by neurons and astrocytes. The percentage is somewhat greater than the value of 14% reported earlier for the awake human occipital cortex during infusions of [2-^{13}C]acetate-Na$^+$ (Lebon *et al*, 2002). The rates of dilution observed during infusions of [1-^{13}C]glucose in previous studies are of similar magnitude but difficult to compare directly, because of the large mass-driven consumption of acetate in this study. Theoretically, administration of ^{13}C-labeled physiologic substrates such as acetate or ketone bodies could be used to evaluate their potential as sources of dilution during ^{13}C-glucose measurements, and such experiments are under way in various laboratories.

Effects of the Sodium Acetate Infusion on Brain Metabolite Levels

The infusion of [2-^{13}C]acetate-Na$^+$ raised plasma levels of sodium, as well as acetate, and the expected hypernatremic condition may have led to the observed rise in glutamate and glutamine concentrations as seen in a previous study of mice (Chowdhury *et al*, 2007). Although sodium levels were not measured in this study, modest increases in plasma sodium of 9% at 20 min and $\sim$16% at 2 h ($[Na^+]_{plasma} < 150$ mmol/L) were observed in mice using a similar infusion protocol scaled for body weight (Chowdhury *et al*, 2007). Acute hypernatremia results in a loss of intracellular water with a slower compensatory increase in cellular osmolytes (Flögel *et al*, 1995). The net accumulation of glutamate and glutamine during the 2 h acetate-Na$^+$ infusion accounted for 2.3 and 1.9 μmol/g, respectively, although their rates of rise occurred slowly (< 0.02 μmol/g/min), equal to $\sim$1.5% of total TCA cycle flux or $\sim$10% of the rate of acetate utilization. The accumulation of amino acids during hypernatremia involves increased synthesis (Flögel *et al*, 1995), which we accommodated in the model by allowing increased mass flow in the astrocytic compartment through anaplerosis (V_{ana}). Osmolyte accumulation in response to hypertonic media is relatively rapid (1 to 2 h) in cultured glial cells but this process appears to be slower *in vivo*. A previous study (Lien *et al*, 1990) reported that brain glutamate and glutamine concentrations were not altered after 2 h of severe hypernatremia ($[Na^+]_{plasma}$, 194 mmol/L) in adult rats, whereas marked increases were seen when hypernatremia was prolonged (7 days). A recent study (Deelchand *et al*, 2009*b*), using an acetate-Na$^+$ infusion similar to that in this study, showed a rise in glutamate (16%) at 2 h, although glutamine levels fell slightly (9%). Thus, we cannot rule out the possibility that acetate also contributed to the rise in glutamate and glutamine, although the similarity to rates of glutamate–glutamine cycling and the neuronal TCA cycle rate obtained with [1-^{13}C]glucose (Patel *et al*, 2005) suggest that kinetic effects of sodium elevations were small.

With knowledge of the transport kinetics, particularly the functional dependence of V_{ac} on blood acetate concentration, it should be possible to measure metabolic fluxes using significantly lower blood acetate concentrations (and reduced sodium load), as long as transporter characteristics can be assumed constant with regard to the condition being studied. Of course, when changes in transport constants are suspected, experimental procedures similar to this study can be used in their evaluation.

Conclusions

The utilization of acetate specifically by astrocytes provides a probe of astrocytic function *in vitro* and *in vivo*. The present analysis of ^{13}C-labeled glutamate and glutamine, and brain acetate concentrations under kinetic and steady-state conditions *in vivo* has provided measurements of kinetics of saturable transport and utilization in the anesthetized rat. The two-compartment (neuron/astrocyte) analysis revealed that intracerebral utilization is saturated at low levels of brain acetate, whereas transport capacity greatly surpasses the capacity for utilization. It was impossible to obtain close fits to the ^{13}C labeling time courses of glutamate and glutamine simultaneously with the acetate labeling time courses unless a small distribution space was permitted; the distribution space that yielded the best fits was 0.32 mL/g, which approximates astrocytic cell volume and the extracellular space in the brain.

There are practical consequences of these findings. Under conditions of significantly elevated plasma acetate, brain acetate utilization becomes saturated, whereas at physiologic levels, the saturability for transport and utilization are both likely to play significant roles in determining consumption. In turn, conditions that increase plasma acetate levels in naturally occurring conditions are likely to lead to increased consumption by the brain.

Acknowledgements

We thank Terry Nixon and Scott McIntyre of the MRRC Engineering Core for maintenance of the NMR spectrometer, Peter Brown for design and fabrication of the NMR probe and transceiver coils, and Bei Wang for animal surgery. This work was supported by grants from the National Institutes of Health: R01 DK027121 (KLB), R01 NS037527 (DLR), and K02 AA13430, P50 AA12870, R01 DA021785, P30 NS-052519, and R21 AA018210 (GFM).

Conflict of interest

The authors declare no conflict of interest.

References

Alcolea A, Carrera J, Medina A (1999) A hybrid Marquadrt-Simulated Annealing method for solving the groundwater inverse problem. Calibration and reliability in groundwater modeling. In: *Proceedings of the ModelCARE 999 Conference*, Zürich, Switzerland, September 1999. IAHS Publication number 265, 2000, pp 157–63

Badar-Goffer RS, Bachelard HS, Morris PG (1990) Cerebral metabolism of acetate and glucose studied by ^{13}C-n.m.r. spectroscopy. A technique for investigating metabolic compartmentation in the brain. *Biochem J* 266:133–9

Baethmann A, Steude U, Horsch S, Brendel W (1970) The thiosulphate (^{35}S) space in the CNS of rats after ventriculo-cisternal perfusion. *Pflugers Arch* 316: 51–63

Bergersen L, Rafiki A, Ottersen OP (2002) Immunogold cytochemistry identifies specialized membrane domains for monocarboxylate transport in the central nervous system. *Neurochem Res* 27:89–96

Brand A, Richter-Landsberg C, Leibfritz D (1997) Metabolism of acetate in rat brain neurons, astrocytes and cocultures: metabolic interactions between neurons and glia cells, monitored by NMR spectroscopy. *Cell Mol Biol* 43:645–57

Broer S, Brookes N (2001) Transfer of glutamine between astrocytes and neurons. *J Neurochem* 77:705–19

Buschiazzo PM, Terrell EB, Regen DM (1970) Sugar transport across the blood-brain barrier. *Am J Physiol* 219:1505–13

Cerdán S, Kunnecke B, Seelig J (1990) Cerebral metabolism of [1,2-$^{13}C_2$]acetate asdetected by *in vivo* and *in vitro* ^{13}C NMR. *J Biol Chem* 265:12916–26

Choi I-Y, Lei H, Gruetter R (2002) Effect of deep pentobarbital anesthesia on neurotransmitter metabolism *in vivo*: On the correlation of total glucose consumption with glutamatergic action. *J Cereb Blood Flow Metab* 22:1343–51

Chowdhury GMI, Gupta M, Gibson KM, Patel AB, Behar KL (2007) Altered cerebral glucose and acetate metabolism in succinic semialdehyde dehydrogenase-deficient mice: evidence for glial dysfunction and reduced glutamate/glutamine cycling. *J Neurochem* 103: 2077–91

Cruz NF, Lasater A, Zielke HR, Dienel GA (2005) Activation of astrocytes in brain of conscious rats during acoustic stimulation: acetate utilization in working brain. *J Neurochem* 92:934–47

de Graaf RA, Pan JW, Telang F, Lee JH, Brown P, Novotny EJ, Hetherington HP, Rothman DL (2001) Differentiation of glucose transport in human brain gray and white matter. *J Cereb Blood Flow Metab* 21:483–92

de Graaf RA, Brown PB, Mason GF, Rothman DL, Behar KL (2003) Detection of [1,6-$^{13}C_2$]-glucose metabolism in rat brain by *in vivo* ^{1}H-[^{13}C]-NMR spectroscopy. *Magn Reson Med* 49:37–46

Deelchand DK, Nelson C, Shestov AA, art¡urbil K, Henry PG (2009*a*) Simultaneous measurement of neuronal and glial metabolism in rat brain *in vivo* using co-infusion of [1,6-13C2]glucose and [1,2-13C2]acetate. *J Magn Reson* 196:157–63

Deelchand DK, Shestov AA, Koski DM, Ugurbil K, Henry P-G (2009*b*) Acetate transport and utilization in the rat brain. *J Neurochem* 109(Suppl 1):46–54

Dimmer KS, Friedrich B, Lang F, Deitmer JW, Broer S (2000) The low-affinity monocarboxylate transporter MCT4 is adapted to the export of lactate in highly glycolytic cells. *Biochem J* 350(Pt 1):219–27

Fitzpatrick SM, Hetherington HP, Behar KL, Shulman RG (1990) The flux from glucose to glutamate in the rat brain *in vivo* as determined by ^{1}H-observed, ^{13}C-edited NMR spectroscopy. *J Cereb Blood Flow Metab* 10:170–9

Flögel U, Niendorf T, Serkowa N, Brand A, Henke J, Leibfritz D (1995) Changes in organic solutes, volume, energy state, and metabolism associated with osmotic stress in a glial cell line: a multinuclear NMR study. *Neurochem Res* 20:793–802

Fujino T, Kondo J, Ishikawa M, Morikawa K, Yamamoto TT (2001) Acetyl-CoA synthetase 2, a mitochondrial matrix enzyme involved in the oxidation of acetate. *J Biol Chem* 276:11420–6

Gerhart DZ, Enerson BE, Zhdankina OY, Leino RL, Drewes LR (1997) Expression of monocarboxylate transporter MCT1 by brain endothelium and glia in adult and suckling rats. *Am J Physiol* 273:E207–13

Gjedde A, Crone C (1975) Induction processes in blood-brain transfer of ketone bodies during starvation. *Am J Physiol* 229:1165–9

Gjedde A, Diemer NH (1983) Autoradiographic determination of regional brain glucose content. *J Cereb Blood Flow Metab* 3:303–10

Gruetter R (1993) Automatic, localized *in vivo* adjustment of all first- and second-order shim coils. *Magn Reson Med* 29:804–11

Gruetter R, Seaquist ER, Ugurbil K (2001) A mathematical model of compartmentalized neurotransmitter metabolism in the human brain. *Am J Physiol Endocrinol Metab* 281:E100–12

Halestrap AP, Wang X, Poole RC, Jackson VN, Price NT (1997) Lactate transport in heart in relation to myocardial ischemia. *Am J Cardiol* 80:17A–25A

Hassel B, Sonnewald U, Unsgard G, Fonnum F (1994) NMR spectroscopy of cultured astrocytes: effects of glutamine and the gliotoxin fluorocitrate. *J Neurochem* 62:2187–94

Hawkins RA, Mans AM (1983) Intermediary metabolism of carboyhdrates and other fuels. I. In: *Biochem J* (Lajtha A, ed), Vol. 122. New York, NY: Plenum Press, 259–94

Hertz L (2004) Intercellular metabolic compartmentation in the brain: past, present and future. *Neurochem Int* 45:285–96

Ikeda Y, Yamamoto J, Okamura M, Fujino T, Takahashi S, Takeuchi K, Osborne TF, Yamamoto TT, Ito S, Sakai J (2001) Transcriptional regulation of the murine acetyl-CoA synthetase 1 gene through multiple clustered binding sites for sterol regulatory element-binding proteins and a single neighboring site for Sp1. *J Biol Chem* 276:34259–69

Kuhr WG, van den Berg CJ, Korf J (1988) *In vivo* identification and quantitative evaluation of carrier-mediated transport of lactate at the cellular level in the striatum of conscious, freely moving rats. *J Cereb Blood Flow Metab* 8:848–56

Lebon V, Petersen KF, Cline GW, Shen J, Mason GF, Dufour S, Behar KL, Shulman GI, Rothman DL (2002) Astroglial contribution to brain energy metabolism in humans revealed by ^{13}C nuclear magnetic resonance spectroscopy: elucidation of the dominant pathway for neurotransmitter glutamate repletion and measurement of astrocytic oxidative metabolism. *J Neurosci* 22:1523–31

Lien Y-H, Shapiro JI, Chan L (1990) Effects of hypernatremia on organic osmoles. *J Clin Invest* 85:1427–35

Ling L, Tolhurst DJ (1983) Recovering the parameters of finite mixtures of normaldistributions from a noisy record: an empirical comparison of different estimating procedures. *J Neurosci Methods* 8:309–33

Luong A, Hannah VC, Brown MS, Goldstein JL (2000) Molecular characterization of human acetyl-CoA synthetase, an enzyme regulated by sterol regulatory element-binding proteins. *J Biol Chem* 275:26458–66

Manning Fox JE, Meredith D, Halestrap AP (2000) Characterisation of human monocarboxylate transporter 4 substantiates its role in lactic acid efflux from skeletal muscle. *J Physiol* 529(Pt 2):285–93

Mason GF, Rothman DL, Behar KL, Shulman RG (1992) NMR determination of the TCA cycle rate and alpha-ketoglutarate/glutamate exchange rate in rat brain. *J Cereb Blood Flow Metab* 12:434–47

Minchin MC, Beart PM (1975) Compartmentation of amino acid metabolism in the rat dorsal root ganglion; a metabolic and autoradiographic study. *Brain Res* 83:437–49

Oldendorf WH (1973) Carrier-mediated blood-brain barrier transport of short-chain monocarboxylic organic acids. *Am J Physiol* 224:1450–3

Oz G, Berkich DA, Henry P-G, Xu Y, LaNoue K, Hutson SM, Gruetter R (2004) Neuroglial metabolism in the awake rat brain: CO2 fixation increases with brain activity. *J Neurosci* 24:11273–9

Pardridge WM, Oldendorf WH (1977) Transport of metabolic substrates through the blood-brain barrier. *J Neurochem* 28:5–12

Patel AB, de Graaf RA, Mason GF, Rothman DL, Shulman RG, Behar KL (2005) The contribution of GABA to glutamate/glutamine cycling and energy metabolism in the rat cortex *in vivo*. *Proc Natl Acad Sci USA* 102:5588–93

Reijnierse GL, Veldstra H, Van den Berg CJ (1976) Radioassay of acetyl-CoA synthetase, propionyl-CoA synthetase and butyryl-CoA synthetase in brain. *Anal Biochem* 72:614–22

Serres S, Bezancon E, Franconi J-M, Merle M (2007) Brain pyruvate recycling and peripheral metabolism: an NMR analysis *ex vivo* of acetate and glucose metabolism in the rat. *J Neurochem* 101:1428–40

Serres S, Raffard G, Franconi J-M, Merle M (2008) Close coupling between astrocytic and neuronal metabolisms to fulfill anaplerotic and energy needs in the rat brain. *J Cereb Blood Flow Metab* 28:712–24

Shen J, Rothman DL, Behar KL, Xu S (2009) Determination of the glutamate-glutamine cycling flux using two-compartment dynamic metabolic modeling is sensitive to astroglial dilution. *J Cereb Blood Flow Metab* 29:108–18

Sibson NR, Mason GF, Shen J, G.W. C, Herskovits A.Z., Wall JE, Behar KL, Rothman DL, Shulman RG (2001) *In vivo* (13)C NMR measurement of neurotransmitter glutamate cycling, anaplerosis and TCA cycle flux in rat brain during hyperammonemia. *J Neurochem* 76:975–89

Sonnewald U, Westergaard N, Schousboe A, Svendsen JS, Unsgard G, Petersen SB (1993) Direct demonstration by [^{13}C]NMR spectroscopy thatglutamine from astrocytes is a precursor for GABA synthesis in neurons. *Neurochem Int* 22:19–29

Terasaki T, Takakuwa S, Moritani S, Tsuji A (1991) Transport of monocarboxylic acids at the blood-brain barrier: studies with monolayers of primary cultured bovine brain capillary endothelial cells. *J Pharmacol Exp Ther* 258:932–7

van den Berg CJ, Garfinkel D (1971) A stimulation study of brain compartments. Metabolism of glutamate and related substances in mouse brain. *Biochem J* 123:211–8

Waniewski RA, Martin DL (1998) Preferential utilization of acetate by astrocytes is attributable to transport. *J Neurosci* 18:5225–33

Williams V, Grossman RG, Edmunds SM (1980) Volume and surface area estimates of astrocytes in the sensorimotor cortex of the cat. *Neuroscience* 5:1151–9

Supplementary Information accompanies the paper on the *Journal of Cerebral Blood Flow and Metabolism* website (http://www.nature.com/jcbfm)